Chapter(IV)
Results and discussion

Chapter (IV)

Results and discussion

The present work is devoted to the study of the flow of a viscoelastic fluid of grade two confined in the annular region between two rotating confocal ellipsoids theoretically . The velocity field, up to a second-order within the frame of retarded motion approximation, is performed. This field is being a superposition of a first- order primary flow distributed uniformly around the axis of rotation and a secondary flow which is every where perpendicular to the streamlines of the primary flow . The problem is solved for the first and the second- order of approximation.

(1). First- order approximation

According to the perturbation technique employed in chapter two in order to determine the velocity field in the problem under consideration , the first term is specified by two partial differential equations ; namely :

(i) The harmonic *(Laplacian)* vector equation

$$\nabla^2(W_1(\zeta,\theta)\hat{\varphi}) = 0 \quad , \tag{2-19}$$

with its boundary conditions

$$\underline{\dot{x}}\big|_{\zeta=\zeta_1} = \hat{\varphi}\Omega_1 h_\varphi(\zeta_1,\theta),$$

$$\underline{\dot{x}}\big|_{\zeta=\zeta_2} = \hat{\varphi}\Omega_2 h_\varphi(\zeta_2,\theta), \tag{2-4}$$

which determines the velocity component in the φ-direction.

(ii)The biharmonic vector equation

$$\nabla^4\left(\frac{c\psi_1(\zeta,\theta)}{h_\varphi}\hat{\varphi}\right)=0 \quad , \tag{2-21}$$

which specifies the first-order stream function , which determines both the ζ and θ components of velocity field.

Equation (2-21) can be decomposed into the two biharmonic scalar functions

$$\nabla^4\left(\frac{c\psi_1\cos\varphi}{h_\varphi}\right)=0 \quad , \tag{2-22}$$

and

$$\nabla^4\left(\frac{c\psi_1\sin\varphi}{h_\varphi}\right)=0 \quad , \tag{2-23}$$

which are subject to the same boundary conditions ; i.e.

$$\psi_1(\zeta,\theta)=\begin{Bmatrix}0\\0\end{Bmatrix} \quad \text{at} \quad \zeta=\begin{Bmatrix}\zeta_1\\\zeta_2\end{Bmatrix} \quad , \tag{2-24}$$

$$\partial_n\psi_1(\zeta,\theta)=\begin{Bmatrix}0\\0\end{Bmatrix} \quad \text{at} \quad \zeta=\begin{Bmatrix}\zeta_1\\\zeta_2\end{Bmatrix} \quad , \tag{2-25}$$

where $\partial_n \equiv \partial_{\underset{\sim}{\zeta}}$ means the normal derivative.

The solution of the Eqs.(2-19) , (2-22) and (2-23) as obtained in chapter two are listed below :

The solution of Eq.(2-19) has the form

$$W_1(\zeta,\theta) = h_\varphi\left(\frac{F(\zeta)-F(\zeta_2)}{F(\zeta_1)-F(\zeta_2)}+\left(\frac{\Omega_2}{\Omega_1}\right)\frac{F(\zeta_1)-F(\zeta)}{F(\zeta_1)-F(\zeta_2)}\right)+0(\Omega_1^2). \qquad (2\text{-}35)$$

The solution which satisfies either of Eqs.(2-22) or (2-23) is

$$\psi_1(\zeta,\theta) = 0 \qquad (2\text{-}29)$$

Hence ,the following discussion is concentrated on the axial primary flow W_1, described by equation (2-35), only . Now some light can be shed on these cases; namely :

Case (1): If the internal ellipsoid ζ_1 is being at rest ; i.e. $\Omega_1 = 0$, and the external ellipsoid ζ_2 rotates with angular velocity Ω_2 , Fig.(4-1) shows that the distribution velocity field $W_1(\zeta,\theta)$ starts from its initial value , $W_1=0$ at $\theta=0$, and then increases monotonically with increasing both of ζ and θ until reaching its maxima at $\theta=\pi/2$ for each ellipsoidal shell $\zeta=$const. After that W_1 decreases monotonically and diminishes at $\theta=\pi$ for all the curves ζ =const.

Case (2): In contrast to case(1), in the present the ellipsoid ζ_2 is being at a stationary state ; i.e. $\Omega_2=0$, while ζ_1 takes its angular velocity Ω_1 . The distribution velocity field W_1 behaves as the same manner as in case (1) with θ while it is inversely proportional to ζ =const. ;Fig.(4-2) .

Case (3): If the two ellipsoids ζ_1 and ζ_2 are rotating with the same angular velocity $\Omega_1 = \Omega_2$,(rigid body motion) the same behavior of W_1 with θ and ζ =const. , as in the case (1) , is obtained but with sharply increasing of W_1 curves ; Fig. (4-3).

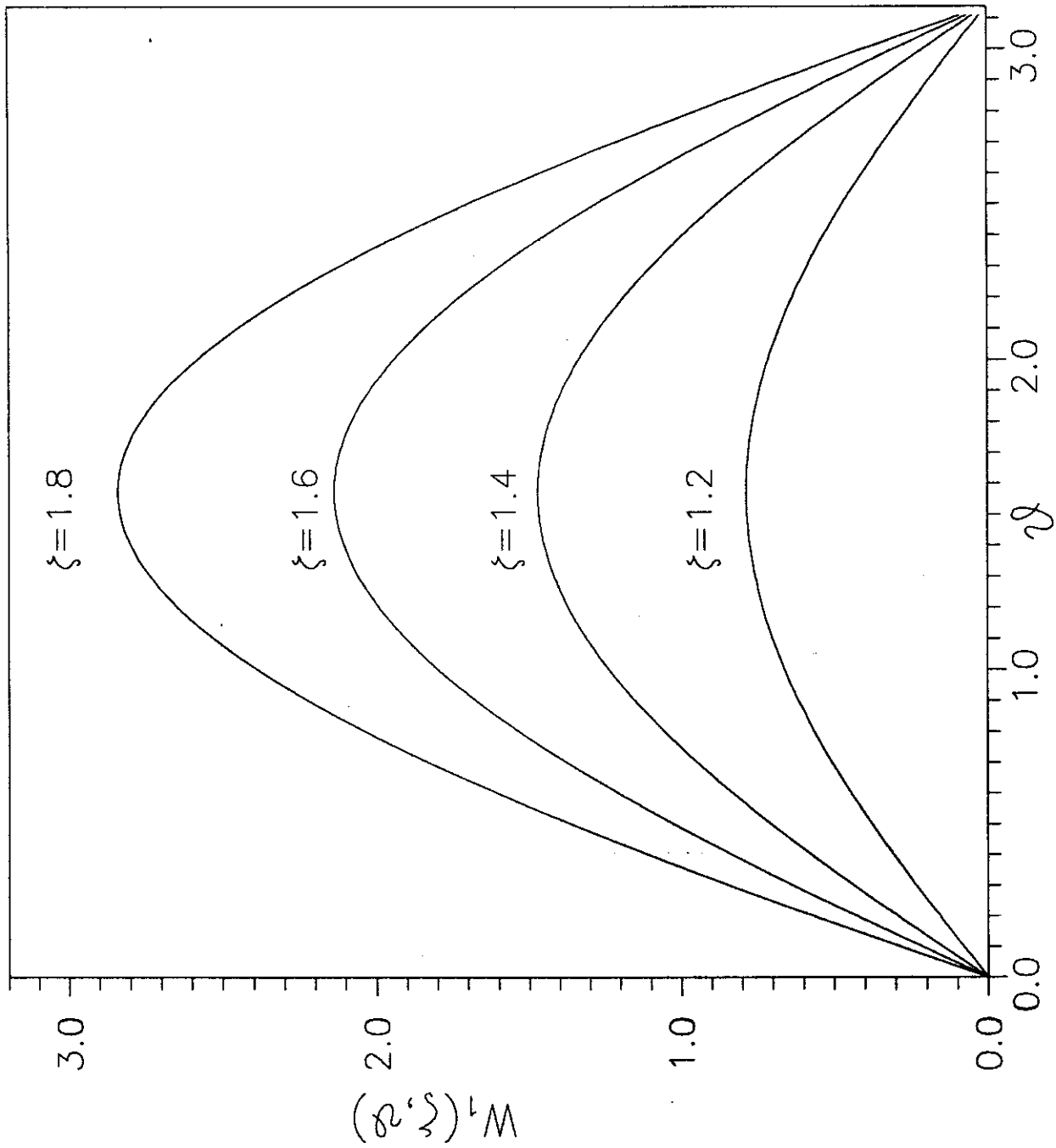

Fig.(4–1) The first–order velocity field distribution $W_1(\zeta,\vartheta)$ versus ϑ at Ω_1=0 while ζ is taken as a parameter.

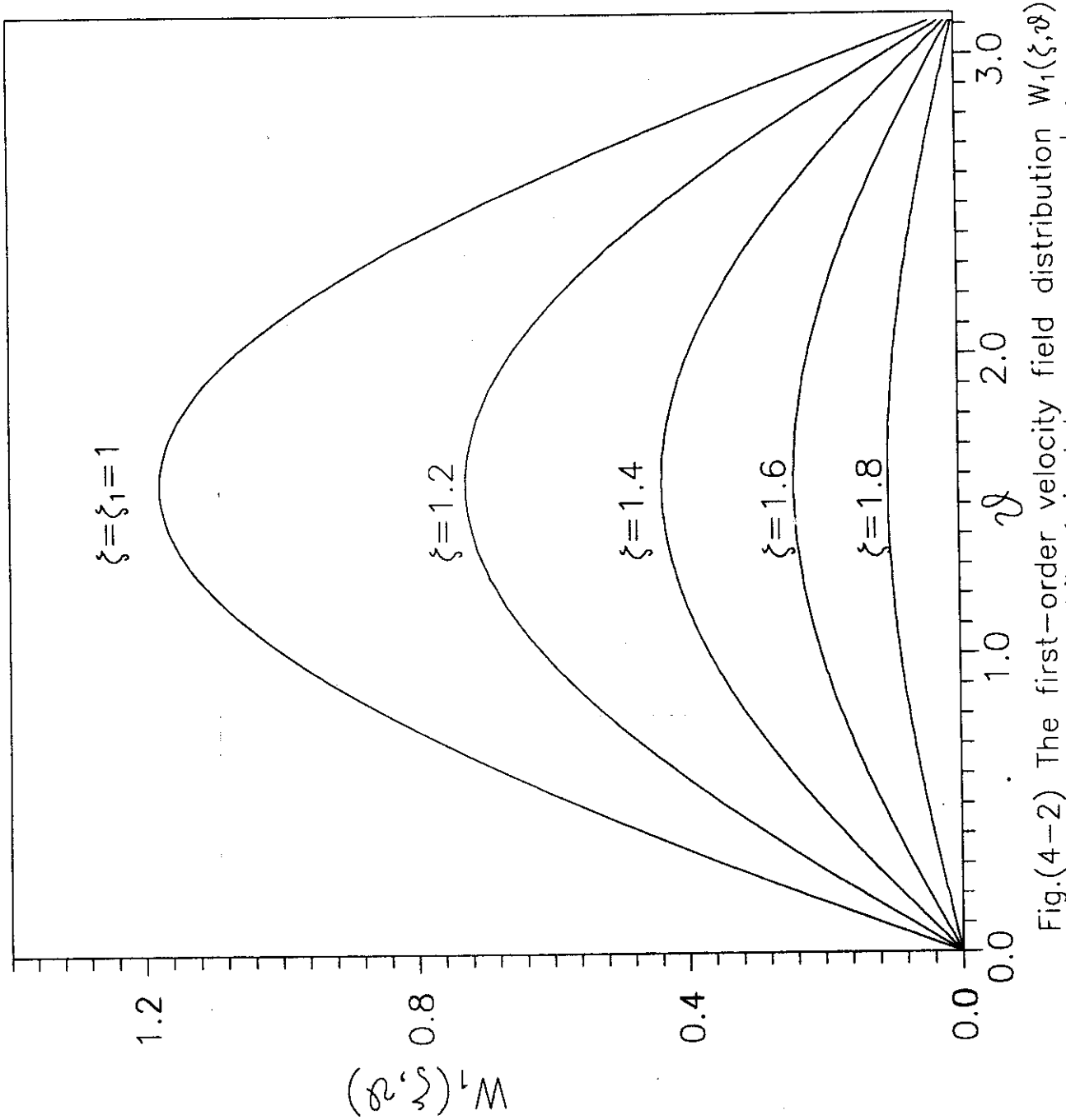

Fig.(4–2) The first–order velocity field distribution $W_1(\xi,\vartheta)$ versus ϑ at $\Omega_2=0$ while ξ is taken as a parameter.

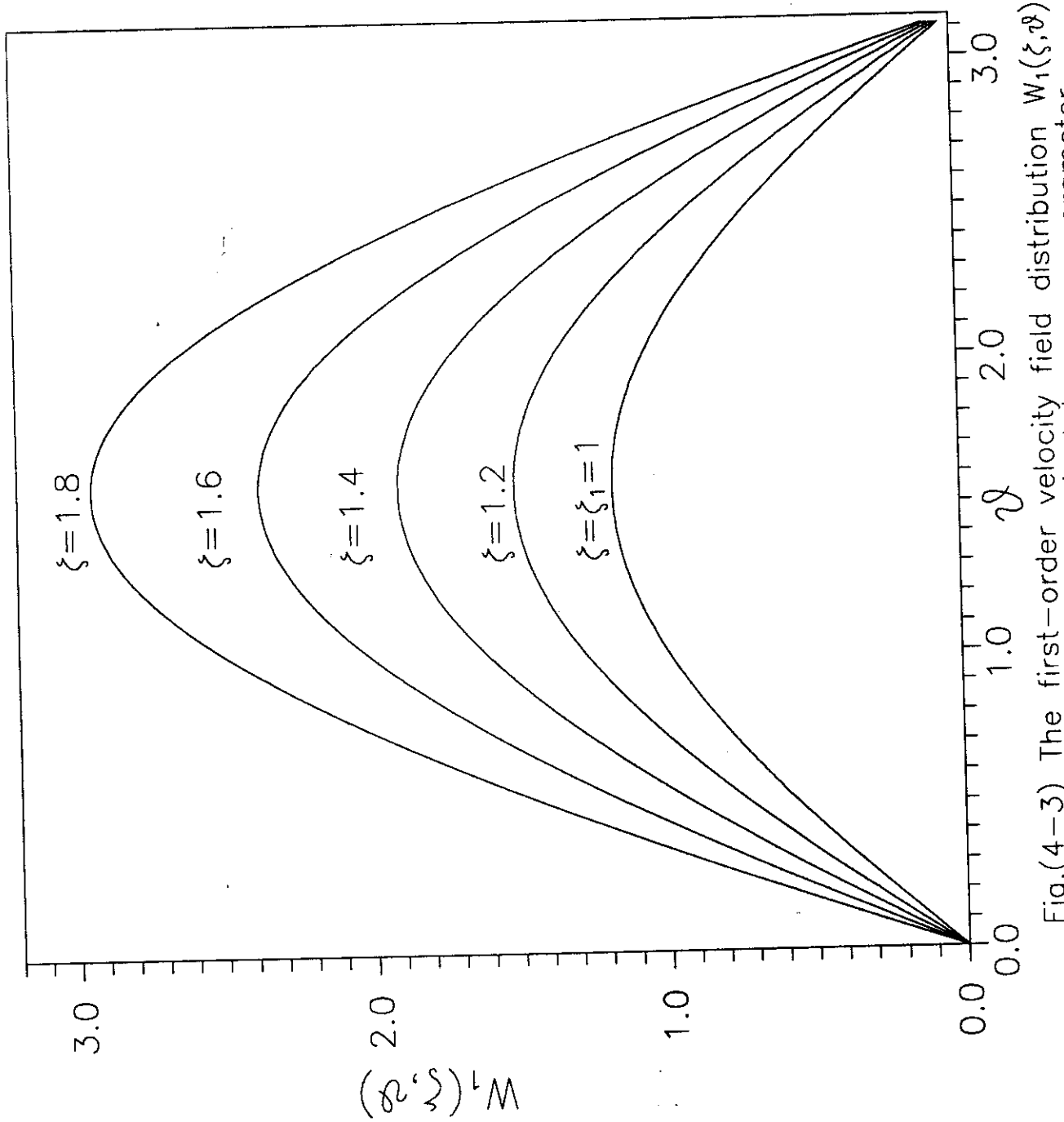

Fig.(4–3) The first–order velocity field distribution $W_1(\xi,\vartheta)$ versus ϑ at $\Omega_1=\Omega_2$ while ξ is taken as a parameter.

Case (4): If the two ellipsoids ζ_1 and ζ_2 are rotating by the same angular velocity but with opposite directions ;i.e. $\Omega_1 = -\Omega_2$, Fig.(4-4) shows that for all values of θ the distribution velocity field W_1 reaches its minimum value ;i.e. $W_1 \approx 0$,at $\zeta = 1.2$ .For $\zeta > 1.2$ the case (1) is being dominant but with –ve values of W_1 while for $\zeta < 1.2$, the case (2) is dominant. Shortly speaking, a dramatic behavior is shown in Fig.(4-4) where for all θ-values, the distribution velocity W_1 decrease with increasing of ζ =const. from its +ve to –ve values for ζ =const. crossing a stagnation shell points at $\zeta = 1.2$.

The behavior of the distribution velocity field W_1 versus ζ for all the last cases $(1 \rightarrow 4)$ at a distinct value $\theta = \pi / 5$ is shown in Fig.(4-5) which is being typically as indicated before in this discussion . Another behavior for W_1 versus θ for all cases $(1 \rightarrow 4)$ at $\zeta = 1.2$ is shown also in Fig.(4-6) with the same results as in Fig.(4-5).

Finally, a compact form of the first order distribution velocity field W_1 which described by Eq. (2-35) is plotted ,at different values of θ with Ω_1=const. and Ω_2=0, versus the dimensionless parameter λ, where $\lambda = (\zeta - \zeta_1)/(\zeta_2 - \zeta_1)$, is shown in Fig.(4-7) .

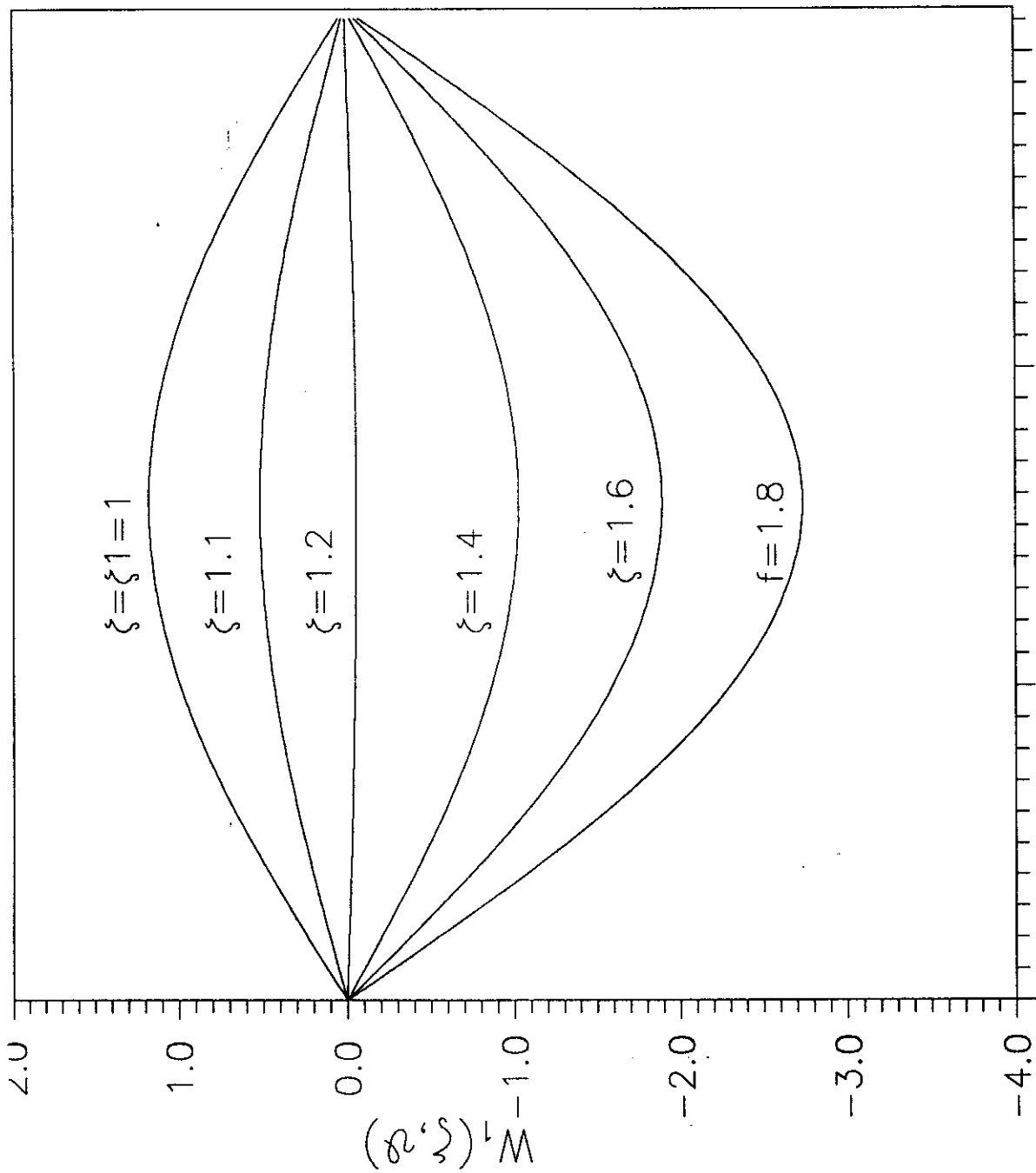

Fig.(4–4) The first–order velocity field distribution $W_1(\zeta,\vartheta)$ versus ϑ at $\Omega_1=-\Omega_2$ while ζ is taken as a parameter.

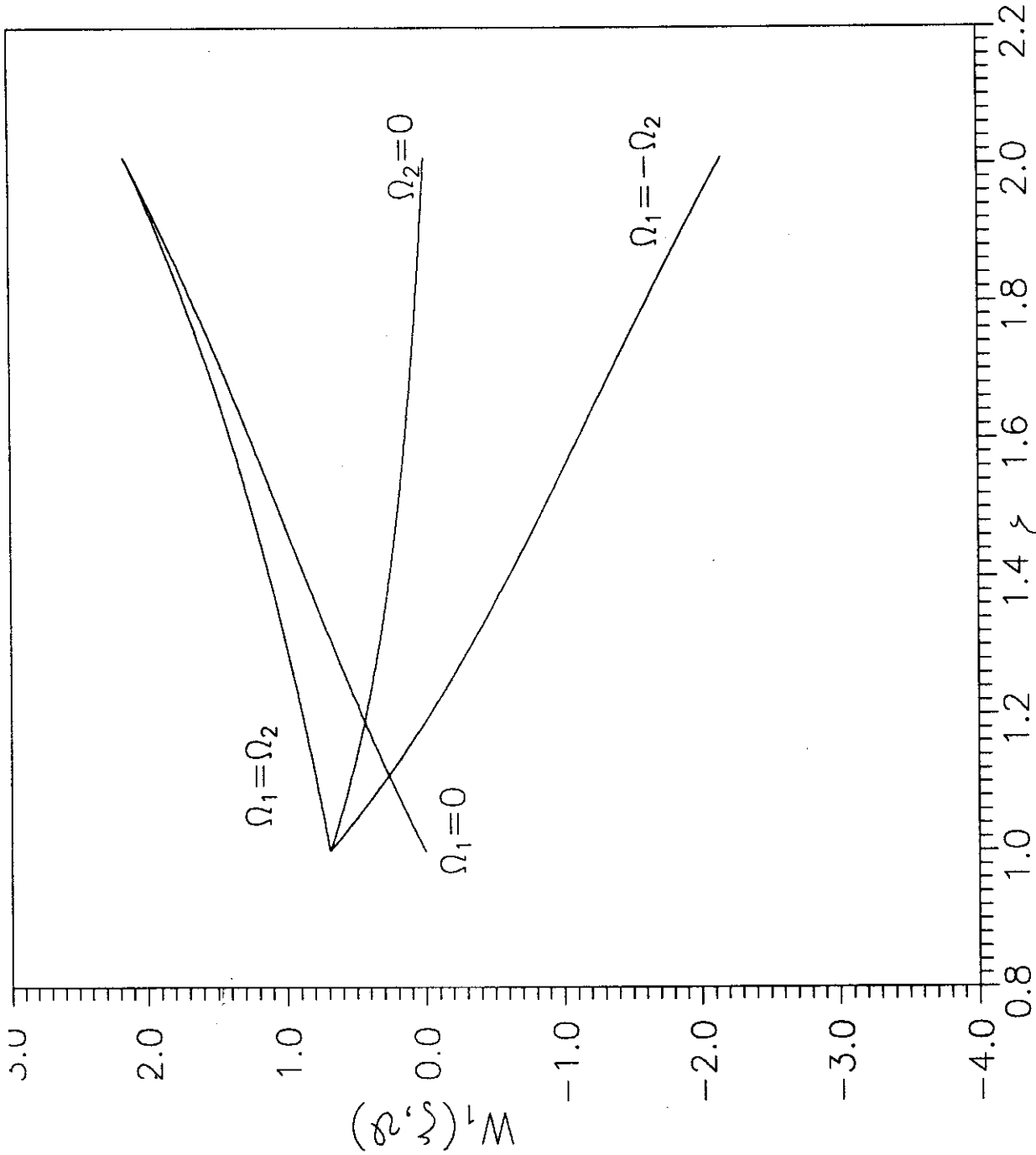

Fig.(4–5) The first–order velocity field distribution $W_1(\zeta,\vartheta)$ versus ζ at $\vartheta=\pi/5$ for different cases of rotation.

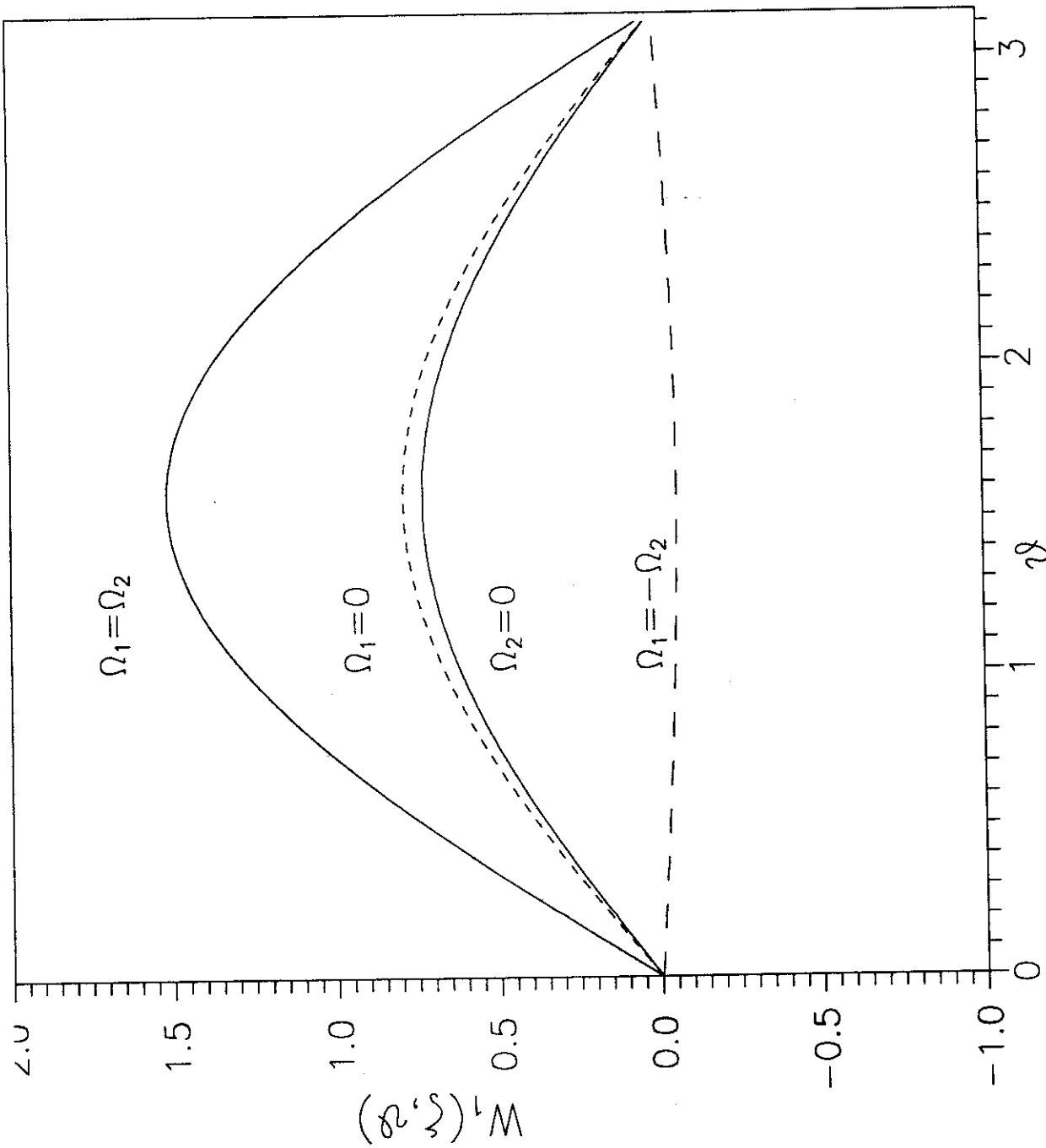

Fig.(4–6) The first–order velocity field distribution $W_1(\xi,\vartheta)$ versus ϑ at $\xi=1.2$ for different cases of rotation.

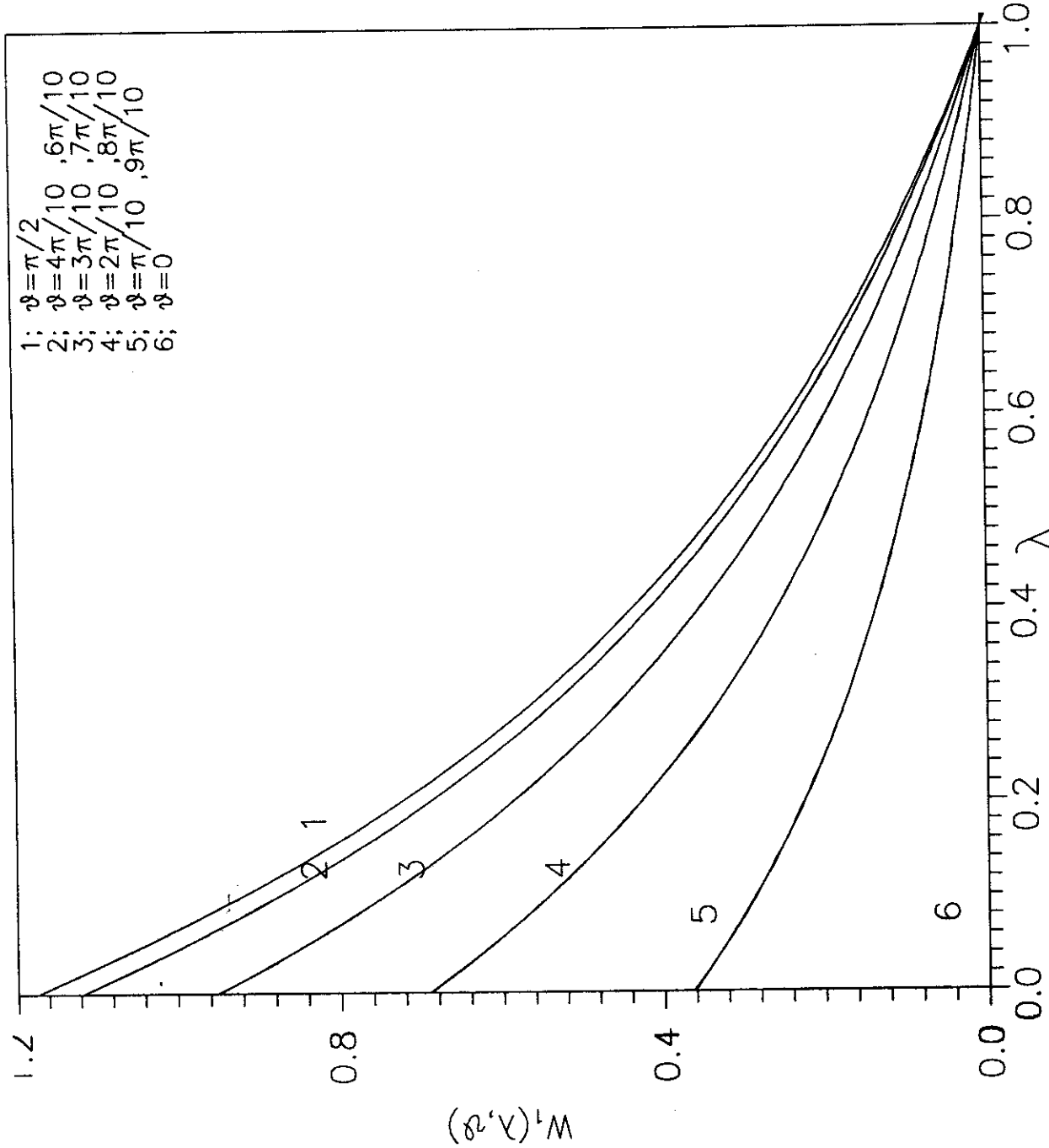

Fig.(4–7) The first–order velocity field distribution $W_1(\lambda,\vartheta)$versus dimensionaless parameter λ at $\Omega_2=0$ while $\vartheta$is taken as a parameter

(2).Second order approximation

Up to this order of approximation the equation of motion reduces to a pair of partial differential equations ; namely :

(i) The harmonic *(Laplacian)* vector equation

$$\nabla^2(W_2(\zeta,\theta)\hat{\varphi})=0, \tag{2-40}$$

with the boundary conditions

$$W_2(\zeta,\theta)=\begin{Bmatrix}0\\0\end{Bmatrix} \quad \text{at} \quad \zeta=\begin{Bmatrix}\zeta_1\\\zeta_2\end{Bmatrix} . \tag{2-41}$$

$$W_{2,\zeta}(\zeta,\theta)=\begin{Bmatrix}0\\0\end{Bmatrix} \quad \text{at} \quad \zeta=\begin{Bmatrix}\zeta_1\\\zeta_2\end{Bmatrix} . \tag{2-42}$$

This boundary value problem has the identity solution

$$W_2(\zeta,\theta)=0. \tag{2-43}$$

all over the domain of motion , and

(ii)The biharmonic vector equation

$$\nabla^4\left(\frac{c\psi_2\hat{\varphi}}{h_\varphi}\right)=\left[\frac{2(\alpha_1+\alpha_2)}{\mu}\rho(\zeta,\theta)\right]\hat{\varphi} \quad , \tag{2-48}$$

with ,

$$\rho(\zeta,\theta)=\left[\frac{16c^2\Omega_1^2\coth\zeta\cot\theta\sin^2\theta}{h^6(F(\zeta_2)-F(\zeta_1))^2\,sh^2\zeta}\left(2+\frac{\sin^2\theta}{sh^2\zeta}\right)\right] ,$$

and its imposed boundary conditions ,

$$\left.\begin{aligned}\psi_2(\zeta,\theta)&=\begin{Bmatrix}0\\0\end{Bmatrix} \quad \text{at} \quad \zeta=\begin{Bmatrix}\zeta_1\\\zeta_2\end{Bmatrix} \quad ,\\ \partial_n\psi_2(\zeta,\theta)&=\begin{Bmatrix}0\\0\end{Bmatrix} \quad \text{at} \quad \zeta=\begin{Bmatrix}\zeta_1\\\zeta_2\end{Bmatrix} \quad .\end{aligned}\right\} \qquad (2-49)$$

which specifies the second - order stream -function $\psi_2(\zeta,\theta)$ which allows the determination of the ζ and θ components of the second-order velocity field.

The solution of Eq.(2-48) is given by

$$\psi_2(\zeta,\theta)=-\frac{32c^2(\alpha_1+\alpha_2)h_\varphi^2}{\mu(F(\zeta_1)-F(\zeta_2))^2}\left\{\begin{aligned}&\frac{\pi}{2}\sin 2\theta\ Q(\zeta)-\frac{2}{3}\cos\theta\ M(\zeta)\\&+q_1+ch\zeta\cos\theta q_2+h_\varphi^2 q_3+h_\varphi^{-2}q_4\end{aligned}\right\} . \qquad (2\text{-}68)$$

where the functions $M(\zeta)$ and $Q(\zeta)$ are respectively given by Eqs.(2-67a) and (2-67b) and the constants q_j ; $j=1,2,...,4$ are respectively given by Eqs.(2-69) , (2-70) ,(2-71)and (2-72).

The present solution of the equation of motion within the second-order approximation gives the stream-function $\psi_2(\zeta,\theta)$ which causes a secondary flow superimposed onto the primary flow which comes from the first-order velocity field $W_1(\zeta,\theta)$.

The cylindrical coordinates ($\rho-z$) are used for plotting the family of streamlines which are satisfying the condition , $\psi_2(\zeta,\theta)=$ constant . In Figure (4-8) the representation of these streamlines in the region of flow $\zeta_1<\zeta<\zeta_2$ are plotted. The map of these streamlines shows a specific symmetry about the axis of rotation; i.e. the z-axis . The inner and outer

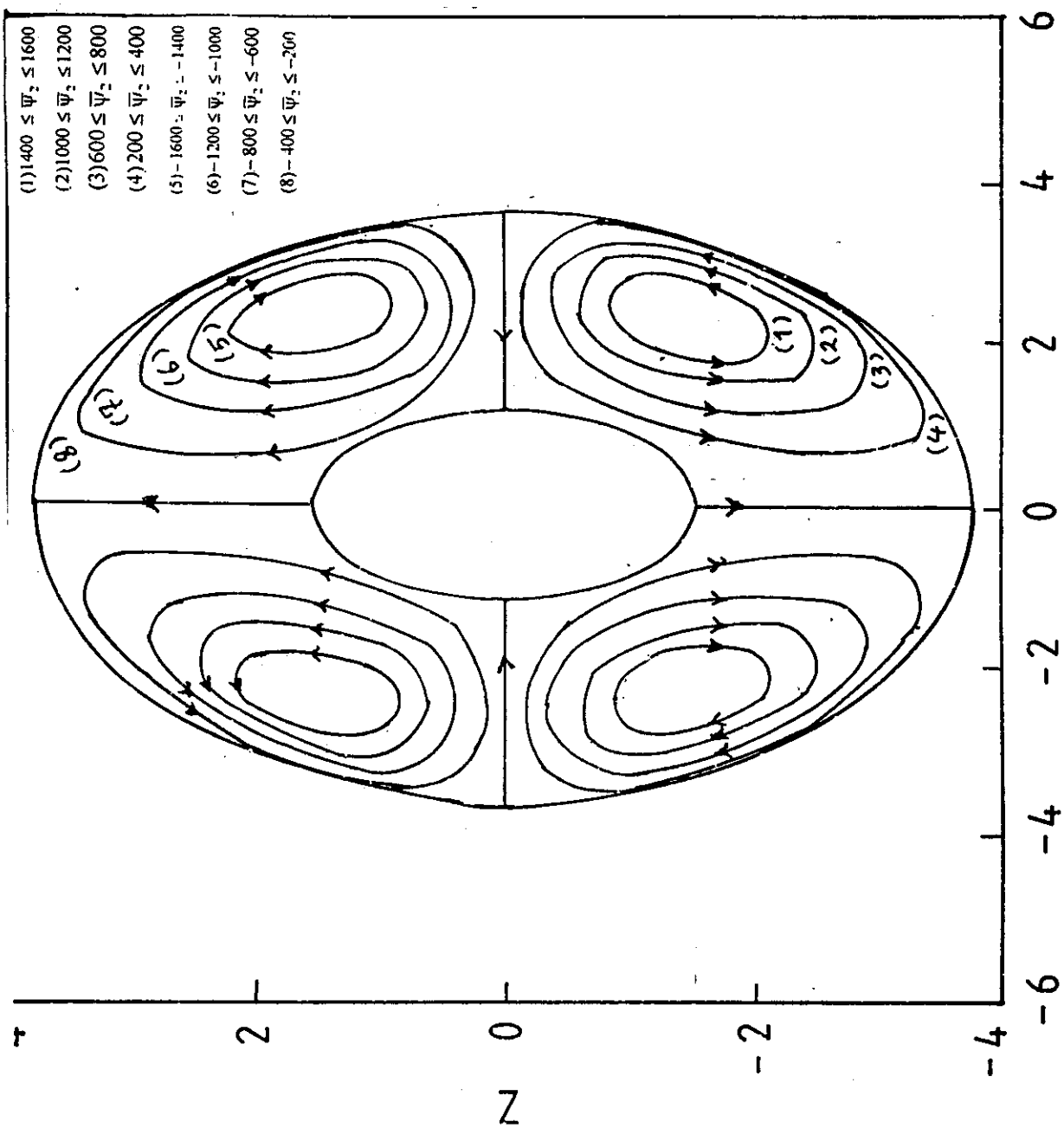

Fig.(4-8) The stream lines of the second-order velocity in ρ -z coordinates.

ellipsoids in the figure are the surfaces representing the equations $\psi_2(\zeta,\theta)=0$.

The streamline pattern of the secondary flow is given by the curves $\psi_2(\zeta,\theta)=$ const. Owing to Eq. (2-68) which can be written in a simple form

$$\psi_2(\zeta,\theta)=\delta\overline{\psi}_2(\zeta,\theta) \quad , \qquad \text{where} \qquad \delta=-\frac{32c^4(\alpha_1+\alpha_2)}{\mu},$$

it must be noticed that these streamlines are the same as the normalized stream function $\overline{\psi}_2(\zeta,\theta)=$ const. Therefore the streamline pattern of the secondary flow depends only on the geometrical cross –section of the flow region and is the same for all viscoelastic second-order fluids, as long as terms of order $O(\Omega^3)$ can be neglected.

Inspection of these streamlines show that $\overline{\psi}_2$ is being symmetric about the axis connecting the foci of the two ellipsoids ; i.e. about the z-axes. Moreover , $\overline{\psi}_2$, is divided into four groups. Every two of them, which are symmetric with one another, are lying around the +ve values of the z-axis and ***are being positive or negative with respect to their correspondence two symmetrical groups,*** which they are lying around the –ve values of the z-axes, ***in accordance with +ve or –ve value of the constant*** δ ***and vice versa*** .

The general streamlines of the fluid particles due to both of the primary and secondary flows can be visualized by combining the primary motion , which takes a closed path about the z-axis ,and the loops of the streamlines mapped onto ρ z-plane . In view of a specific particle located in a specific circular primary path , when exposed to the additional

secondary motion it will draws a closed loop .Since the secondary motion is usually much slower than the primary one ,the secondary loop is exposed to be closed after several primary rotations. Because of the number of points for one value of $\overline{\psi}_2$ is not enough to draw the loop we take the average value ; i.e. $\overline{\psi}_2 \pm 15\ \%$.

Based on the last calculation , stress components and therefore the resultant forces and torques on the boundaries are determined . The resultant torque and force are expressed in terms of geometrical parameters , which are appropriate for practical purposes . Therefore , the first measurable quantity is the torque acting on the outer ellipsoid ζ_2 which is given by

$$M(\zeta_2,\theta)=\frac{16\pi\mu\Omega_1}{3(F(\zeta_1)-F(\zeta_2))}+\frac{32\pi(\beta_2+\beta_3)\Omega_1^3c^3}{3\sinh^4\zeta_2(F(\zeta_1)-F(\zeta_2))^3}(4-6\sinh^2\zeta_2) \quad . \quad (3\text{-}42)$$

Finally, the calculation of the resultant torque up to the third-order , Eq.(3-42), show that there are two torque components namely; the primary viscous term and a third-order correction term which depends on the combined material parameter $(\beta_2+\beta_3)$.

For practical purposes the first term of the resultant torque which is given by Eq. (3-42) may be expressed as

$$M|_{\zeta_2}=\frac{16\pi\mu\Omega_1}{\left[\frac{b_1^2-3a_1^2}{a_1^3b_1^2}-\frac{b_2^2-3a_2^2}{a_2^3b_2^2}\right]} \quad ,$$

from which the coefficient of viscosity μ can be determined .

In the case of concentric spheres, as a special case , the last equation at $a_1 = b_1 = R_1$ and $a_2 = b_2 = R_2$ is being ,

$$M|_{R_2} = \frac{8\pi\mu\Omega_1 R_1^3 R_2^3}{\left[R_2^3 - R_1^3\right]} \quad ,$$

which is the same result as in the literature [21,46].

From the second term of Eq.(3-42) we can determine the third-order shear viscosity $(\beta_2 + \beta_3)$. Which is being the second measurable quantity in the present work.

We notice that all the components of force at ζ_2 are vanished; i.e.

$\underline{F}(\zeta_2, \theta) = \underline{0}$.

as indicated before by Eq. (3-39) which is consistent with the geometrical symmetry of the present boundary value problem .